Proc. Natl. Acad. Sci. USA
Vol. 86, pp. 1071–1075, February 1989
Neurobiology

Organization of corticocortical connections in human visual cortex

ANDREAS BURKHALTER AND KERRY L. BERNARDO

Department of Neurology and Neurological Surgery (Neurosurgery) and McDonnell Center for Studies of Higher Brain Function, Box 8057, Washington University School of Medicine, Saint Louis, MO 63110

Communicated by Clinton N. Woolsey, October 26, 1988

ABSTRACT **Clinical and psychophysical observations indicate that the visual cortex is critical for the perception of color, form, depth, and movement. Little, however, is known about the cortical circuitry that underlies these functions in humans. In an attempt to learn more about these connections, we have traced projections of primary (V1) and secondary (V2) visual cortex in the postmortem, fixed human brain, using the fluorescent dye 1,1′-dioctadecyl-3,3,3′,3′-tetramethylindocarbocyanine perchlorate as an axonal marker. The results show that V1 makes a forward projection to layers 3 and 4 of V2, and V2 projects back to layers 1, 2, 3, 5, and 6 of V1. Some V2 injections also show an input to layer 4B of V1. Projections to 4B probably originate from cytochrome oxidase (CO)-reactive stripes that we have identified in V2. Differential connections between CO-rich (blobs) and CO-poor regions (interblobs) also exist within V1; blobs are connected to blobs and interblobs are connected to interblobs. The results show that the connections in human visual cortex are similar to those of nonhuman primates and that their organization is consistent with the concept of multiple processing streams in the visual system.**

The current understanding of the neuronal mechanisms that underlie the perception of color, form, and visual motion is derived to a large part from anatomical and physiological studies of nonhuman primates. These studies have shown that the visual system is composed of multiple processing streams that originate in the retina and that are linked to different subcortical and cortical areas (1, 2). Little, however, is known about the anatomy of these pathways in humans and their cortical organization remains obscure.

Since Gennari's description of human striate cortex (V1) in 1782 (for review, see ref. 3), progress on understanding the organization of its intracortical connections has been hindered by the limited usefulness of modern pathway tracing techniques in the human brain. In spite of this, important information on the internal organization of visual cortex was obtained from cytoarchitectural studies that revealed cortical layers and areal boundaries (4–8). More recent studies, employing silver impregnation and staining techniques for visualizing cytochrome oxidase (CO) activity, have focused on the organization within layers. Human striate cortex has been shown to contain ocular dominance stripes, CO-rich blobs, and CO-poor interblobs (9, 10). In the area that adjoins human V1, tangential patterns were shown with antibodies to specific antigens (11). These patterns resemble the thick CO-rich stripes in secondary visual cortex (V2) of the monkey, which are known to provide input to the middle temporal area MT (12, 13). In nonhuman primates several of these anatomical features have been associated with different functional streams and their identification in the human visual cortex offered the possibility to study these pathways in the human brain. To this end we injected visual cortex in postmortem, aldehyde-fixed tissue with the neuronal tracer 1,1′-dioctadecyl-3,3,3′,3′-tetramethylindocarbocyanine perchlorate (diI) (14) and related the local connections to the CO-staining patterns in V1 and V2.

The publication costs of this article were defrayed in part by page charge payment. This article must therefore be hereby marked "*advertisement*" in accordance with 18 U.S.C. §1734 solely to indicate this fact.

METHODS

Pieces of occipital lobe containing striate and extrastriate visual cortex were obtained from four human brains (29, 44, 52, and 85 years old, without known neurological disease). Within 14–30 hr postmortem, blocks of tissue were placed in a phosphate-buffered 3% paraformaldehyde solution containing 0.1 M lysine-HCl, 0.8% $NaIO_4$ (15), and 0.8% iodoacetic acid (16) for 24 hr at 4°C. In some cases, after a brief fixation, cortex was unfolded, flattened, and stored in fixative for a total of 24 hr. Striate cortex was identified grossly by the stria of Gennari, and crystals of the fluorescent dye diI (Molecular Probes) were placed with glass micropipettes at multiple sites into V1 and into a ≈1-cm-wide strip of cortex adjoining V1. This part of extrastriate cortex presumably corresponds to the vertical meridian representation of area V2 (17). To allow for intramembranous axonal diffusion of the dye, the injected tissue was stored in phosphate buffer (0.1 M) for 2–8 weeks at 21°C. Subsequently, 60-μm sections were cut on a vibratome in planes parallel or orthogonal to the pial surface. Alternating, floating sections were stained for CO (18) mounted on glass slides, coverslipped with Aquamount (Polyscience), and viewed and photographed under a fluorescence microscope equipped with rhodamine optics. Uninjected tissue was cut on a freezing microtome, and mounted sections were stained for CO. Laminar and areal borders were identified on Nissl- or CO-stained sections (7, 10).

RESULTS

Injection Sites and Neuronal Labeling. Forty-five injections were directed into cortex identified as V1 by the stria of Gennari. Injection sites were verified histologically by the characteristic Nissl-staining pattern of striate cortex (Fig. 1*A*). Thirty-two injections were placed outside V1. Each of these was within ≈1 cm of the V1 border and was therefore considered to be in V2. In many cases areal assignments were confirmed on CO-stained sections, where V1 is distinguished by its regular pattern of darkly stained blobs and pale interblobs in layers 2 and 3 (Fig. 1*B*). Area V2 is identified by the absence of blobs and the presence of CO-rich stripes in layers 3–5 (see Fig. 5*A*).

Injection sites were 0.25-1 mm in diameter and involved different layers (e.g., Fig. 1*C*). Each injection resulted in labeled fibers and cell bodies (Fig. 2*B*), distributed in specific and reproducible laminar and tangential patterns. Many projections could be followed to their terminations in targets up to 6 mm away from the injection site.

Local Projections in V1. The local labeling pattern after a *large* V1 injection involving layers 1–3 is shown in Fig. 1*C*. Fibers in layers 2 and 3 run parallel to the pial surface and terminate in nonuniform fashion 1–2 mm beyond the injection

Abbreviations: diI, 1,1′-dioctadecyl-3,3,3′,3′-tetramethylindocarbocyanine perchlorate; CO, cytochrome oxidase.

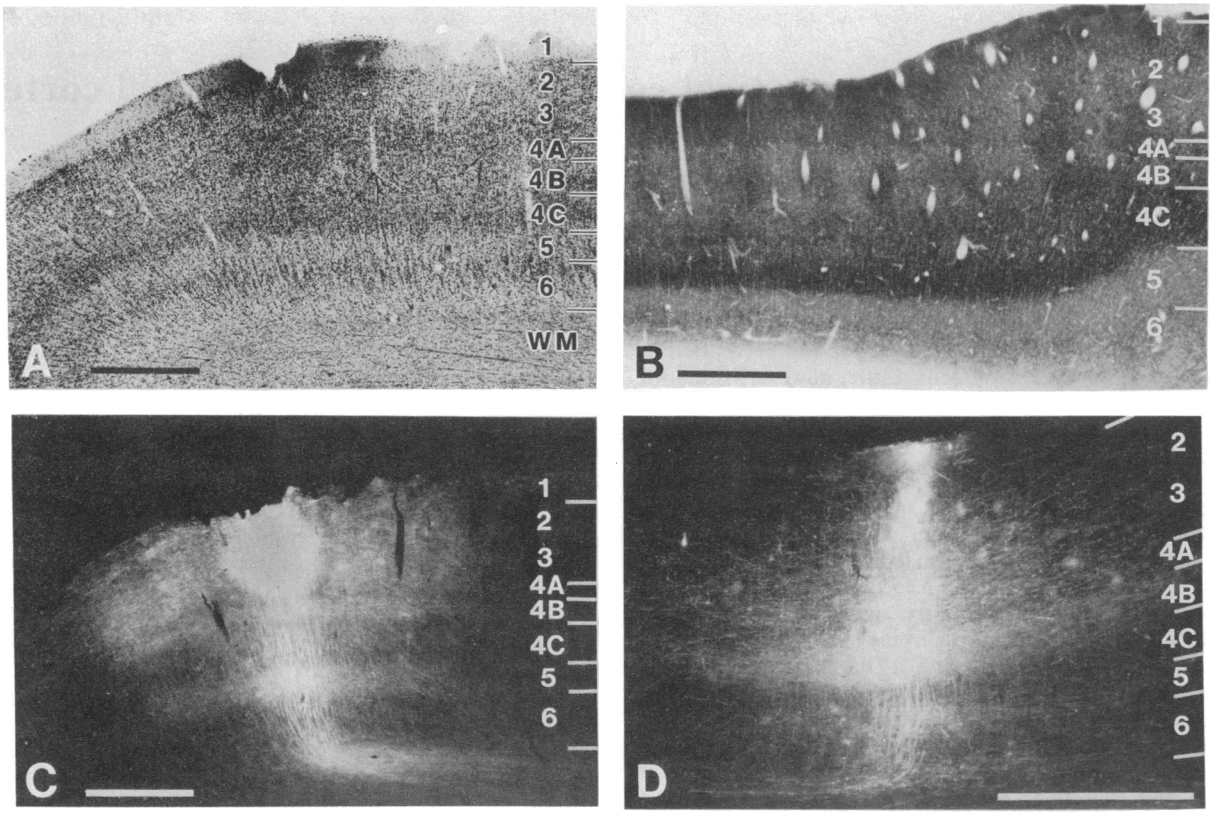

FIG. 1. Identification and local connections of human primary visual cortex (V1). (*A*) Transverse section of V1 stained for Nissl substance, showing cortical layers. (*B*) Transverse section of V1 stained for CO reactivity. The regular pattern of CO-rich and CO-poor regions in layer 3 corresponds to blobs and interblobs, respectively. (*C*) Fluorescence photomicrograph of a section through V1 adjacent to that shown in *A*. Bright spot in layers 1–3 is the dil injection site. Labeling beyond this injection represents fibers, terminals, and cell bodies. Horizontal projections are seen in layers 2, 3, 4B, and 5. Labeled axons stream into the white matter (WM) below layer 6, whereas others interconnect superficial and deep layers. (*D*) Transverse section through V1. dil injection is centered in layers 4B and 4C. Note that fiber labeling pattern differs from that in *C*; horizontal projections in layers 2, 3, and 5 are less extensive and layer 4B labeling is more widespread. (Bars = 1 mm.)

site. Beneath the injection site, layer 4A is unlabeled. As in superficial layers, labeling in layers 4B and 5 spreads wider than the injection site and terminal density waxes and wanes in the horizontal plane. The projection to layer 6 is narrow and weak. Many fibers run vertically between layers, but only a narrow bundle descends from the injection site to the white matter. Similar laminar patterns were previously shown in monkey V1 (19).

Injections largely confined to the stria of Gennari (layers 4B and upper 4C) result in different laminar patterns of labeling than superficial injections (Fig. 1*D*). Fibers rise vertically from the injection site to terminate in a narrow region of layers 4A and 3; horizontal projections in layer 3 are widespread and appear uniform. Descending projections are similar to those seen with more superficial injections and terminate in layers 5 and 6.

Small injections revealed even more distinct projection patterns. Layer 3 injections, for example, result in striking sunburst patterns in the tangential plane (Fig. 2*A*). Fibers radiate away from the injection site and terminate in layers 2 and 3 in clusters 0.3–0.5 mm wide with a center-to-center spacing of 0.6–1 mm. In cases where the injection was

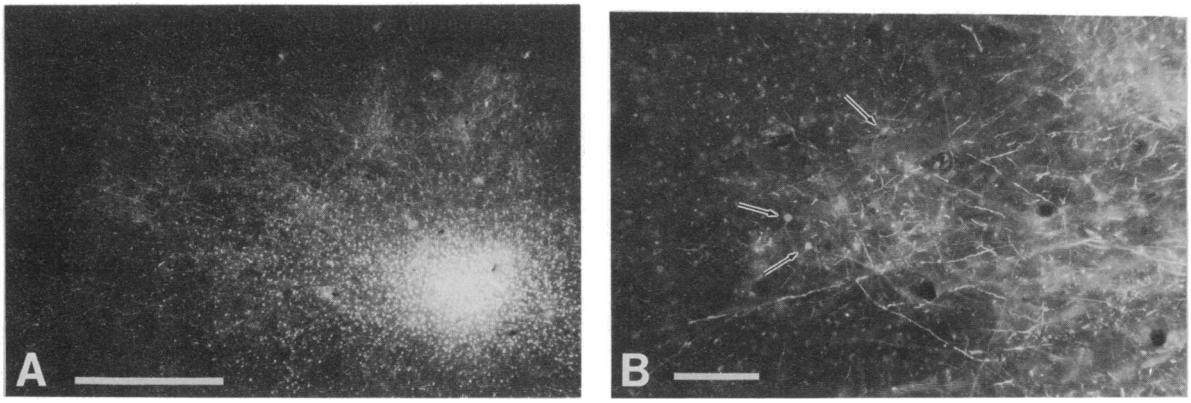

FIG. 2. Local connections within human V1 traced with dil. (*A*) Tangential section through layer 3 of V1 showing clustered projections at 10, 11, 11:30, and 12 o'clock within radius of ≈2 mm of injection site at the lower right. (Bar = 1 mm.) (*B*) High-power picture of cluster of fibers and neuronal cell bodies (arrows), 1.5 mm away from injection site. (Bar = 0.2 mm.)

confined to a blob the projections terminated preferentially within blobs and tended to avoid interblobs (Fig. 3 *A* and *B*). In contrast, after interblob injections (Fig. 3 *C* and *D*) fibers run away from the injection site and, as shown in the example in Fig. 3*C*, traverse a blob, enter an interblob region, and then turn toward the pia to terminate in a narrow column adjacent to another blob. This suggests that the local connections within layers 2 and 3 are highly specific; blobs project to blobs and interblobs project to interblobs.

Connections Between V1 and V2. To study the laminar organization of projections between V1 and V2, we made larger injections into both areas close to the V1/V2 border. With V1 injections, a bundle of fibers would typically enter white matter beneath the injection site, cross the V1/V2 border, and ascend into gray matter of V2 terminating in ≈0.5-mm-wide clusters within layers 3 and 4 (Fig. 4*A*). A large number of fibers also travel horizontally through gray matter to terminate in the same narrow region of V2. V2 injections give rise to a projection pattern in V1 that is different. As shown in Fig. 4*B*, a bundle of labeled fibers descends into white matter, but only a few fibers reenter gray matter after crossing the V1/V2 border. Instead, the vast majority of projection fibers run through gray matter and terminate in layers 1, 2, 3, 4B, 5, and 6, avoiding layers 4A and 4C. The terminals in layers 4B and 5 are distributed in nonuniform fashion, making ≈0.3-mm-wide clusters with a center-to-center spacing of 0.6–1 mm. In superficial layers terminal clusters are less obvious. Not every V2 injection results in the exact same projection pattern in V1. In several cases the projection is lacking a significant termination in layer 4B (Fig. 4*C*).

Local Projections in V2. The findings of clustered projections from V1 to V2 and of the laminar diversity in the projections from V2 to V1 suggest that the tangential organization in V2 is anatomically heterogeneous. Indeed, staining V2 for CO revealed a regular pattern of dark (1–2.75 mm wide) and pale (1.5–2.75 mm wide) stripes running roughly orthogonal to the V1/V2 border (Fig. 5*A*). Although this organization is reminiscent of the CO pattern in V2 of nonhuman primates, which shows thin, thick, and pale stripes (20), more work is needed to determine whether this tripartite organization also exists in humans.

As in the CO-stained material, the local connections in V2 also suggest compartmentalization. Evidence for this is shown in Fig. 5*B*. Here, after a dil injection into superficial V2, terminal clusters are visible in layers 2–5. Interestingly, these terminals are similarly disposed to those in monkey V2 (21); clusters only 0.3–0.5 mm wide are closely spaced and thus differ in size and spacing from the CO stripes. In addition, in the tangential plane the dil-labeled clusters are only slightly elongated and do not form obvious stripe-like arrays (Fig. 5*C*).

DISCUSSION

This report provides evidence that modern neuronal pathway tracing techniques can be used in experimental anatomical studies of the human brain. Although similar approaches have been tried before (22–24), specific connections within and between identified areas of human cerebral cortex have not been described. By using dil as a tracer in combination with CO histochemistry we have shown intracortical con-

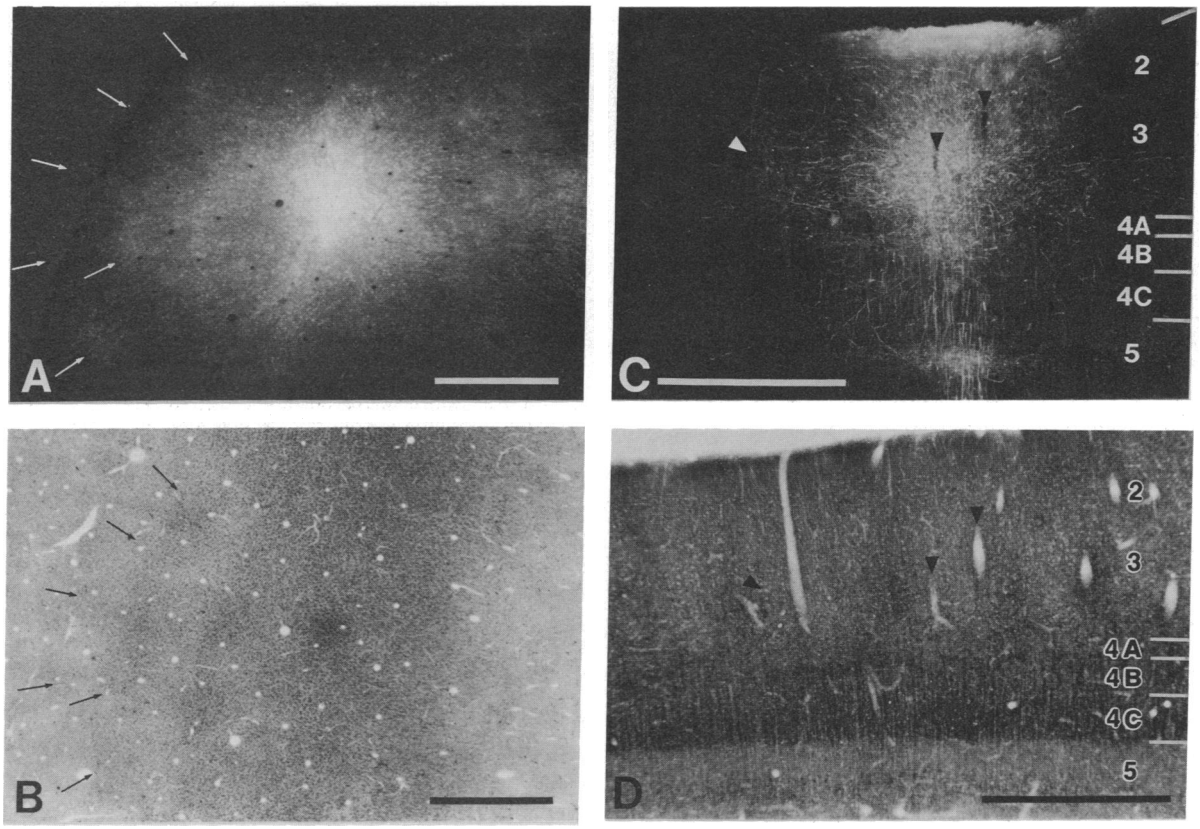

FIG. 3. Specificity of local connections of human V1. (*A*) Tangential section through layer 3 of V1. Rows of clustered projections (arrows) surround the dil injection site (brightest spot in center). (*B*) CO-stained section adjacent to *A*. The dil injection (darkest spot in center) is confined to a blob. The projections are clustered and preferentially go to nearby blobs (arrows). (*C*) Transverse section of V1. dil injection is centered in an interblob in layer 3 (compare corresponding arrowheads in CO-stained section in *D*). Horizontal fibers traverse the blob to the left of injection site and terminate in adjoining interblob. (*D*) CO-stained section adjacent to *C*. Arrowheads indicate corresponding points in *C*. (Bars = 1 mm.)

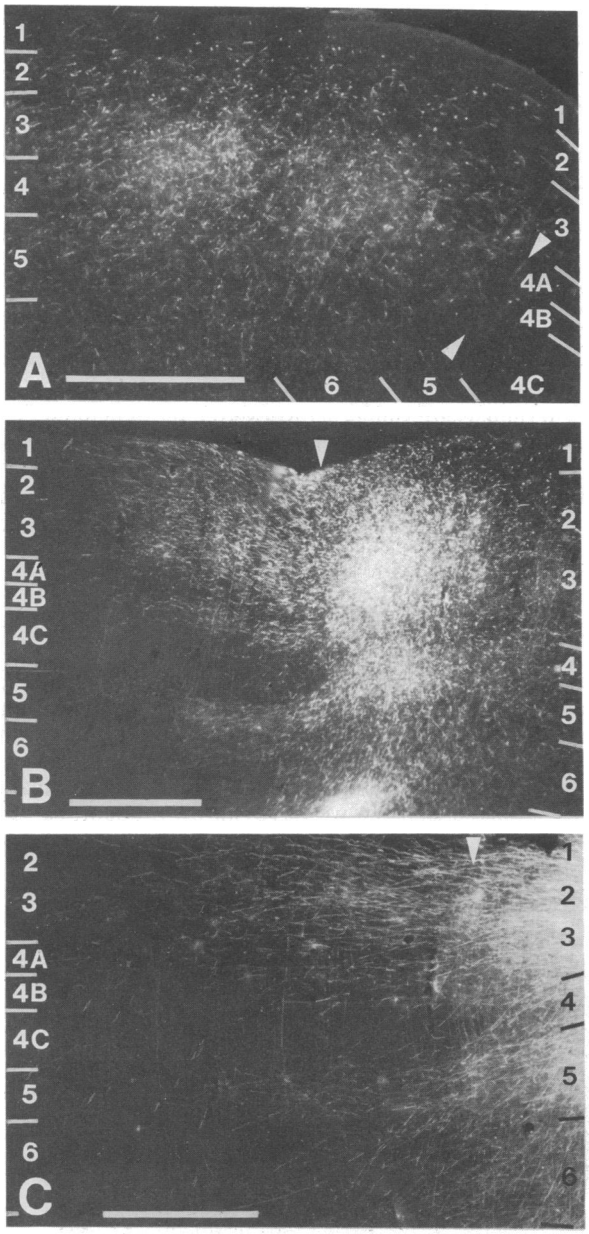

FIG. 4. Connections between V1 and area V2 of human visual cortex, traced with dil. (*A*) Projection from V1 to V2: transverse section from V1/V2 border (arrowheads). Fibers are seen in all layers of V2 (left of arrowheads), but the clustered terminations are restricted to layers 3 and 4. (*B*) Projection from V2 to V1 with terminations in layer 4B of V1: transverse section from V1/V2 border (arrowhead) showing injection into layers 1–5 of V2. Projections to V1 terminate in layers 1, 2, 3, 4B, and 5 of V1 (left of arrowhead). Terminal clusters are most obvious in layers 4B and 5. (*C*) Projection from V2 to V1 without terminations in layer 4B of V1: transverse section from V1/V2 border. V2 injection site is right of arrowhead. Left of arrowhead are projection fibers in layers 1, 2, 3, and 5 of V1. (Bars = 1 mm.)

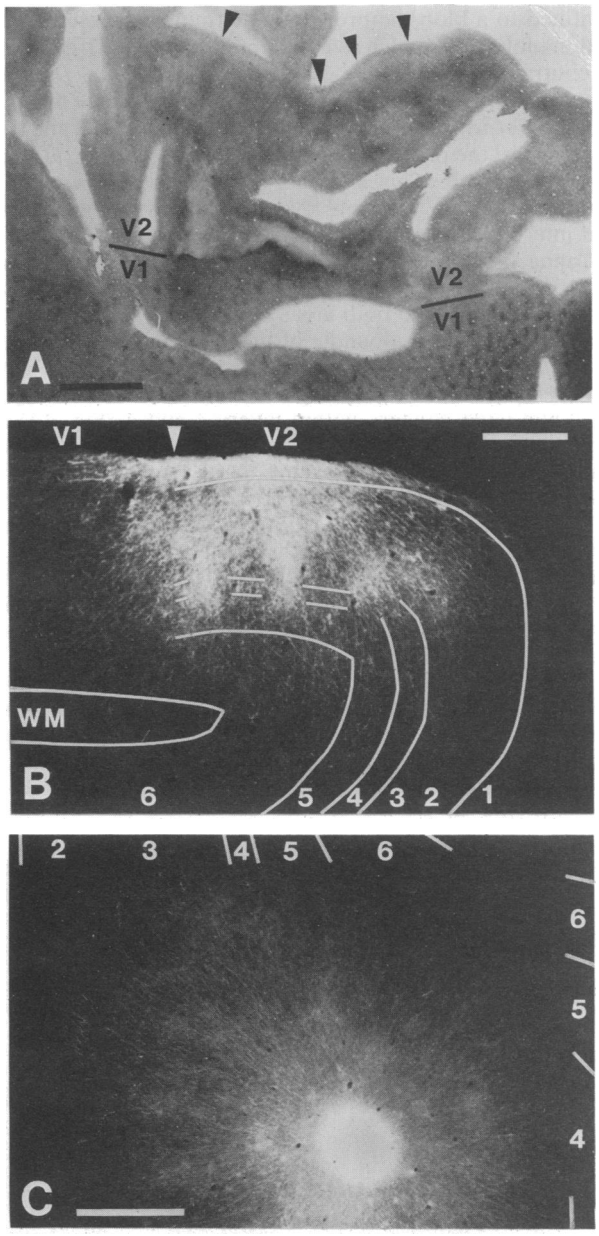

FIG. 5. Intrinsic organization of human V2. (*A*) Tangential section through V1 (bottom half) and V2 (top half) stained for CO. V1/V2 border runs horizontally. V1 shows CO-reactive blobs. V2 shows regular pattern of dark and light stripes that run roughly orthogonal to the V1/V2 border. The width of dark stripes is 1–2.75 mm. (Bar = 5 mm.) (*B*) Transverse section through V2, showing dil-labeled projections within V2. Clustered projections extend from the injection site in layers 1–4 to layers 2–5. Clusters are narrower and more closely spaced than CO stripes in *A*. The arrowhead indicates the V1/V2 border. WM, white matter. (Bar = 1 mm.) (*C*) Oblique section through V2 showing clusters of intrinsic projections that radiate out from the injection site. (Bar = 1 mm.)

nectivity patterns and their relationship to anatomically and presumably also functionally different subdivisions of primary (25) and secondary (12, 13, 26) visual cortex. Although these connections were traced in *fixed* tissue (14), they closely resemble those visualized with *in vivo* axon-tracing techniques in monkeys (27–29). This strongly suggests that this approach will be useful for identifying alterations of neuronal connections associated with aging or neurological disorders. It is likely that it will also provide insights into the organization of functional areas not present in nonhuman brains (e.g., cortical areas that relate to speech).

Recent positron emission tomographical studies suggest that human cortex contains multiple visual areas that are selectively activated during specific tasks that involve vision (30–32). Of these areas, only V1 has been anatomically identified (3). We now report progress toward identification of area V2, demonstrating regular patterns of CO stripes, which are similar but not identical to those in monkey V2 (20, 25). In addition, we have shown that the connections between V1 and V2 are reciprocal and that the input from V1 to V2

terminates in layers 3 and 4, whereas the return projection terminates in upper and lower layers. These asymmetric laminar patterns are known to exist in monkey visual cortex and are thought to represent forward and feedback projections (27, 28, 33). Such connections define the relationships between different areas and indicate the direction of information flow through these areas of cortex (33). Although the picture of interareal connectivity in human visual cortex is incomplete, the laminar organization of the connections between V1 and V2 suggests that visual areas are arranged hierarchically and that V2 represents a processing stage above V1.

Although the link between areas V1 and V2 suggests successive stages of cortical processing from one area to the next, the connectivity patterns between and within areas also provide information about the organization of different processing streams and their interactions (for review, see ref. 1). In monkey striate cortex, the M stream is linked to motion analysis. It flows through layer 4B to thick CO stripes in V2. Thick stripes in turn project back to 4B in V1 (34). We have identified a similar projection from V2 to V1 in humans, although, at present, we do not know for certain whether this layer 4B projection originates in thick CO stripes. The results show that the presence of the layer 4B projection depends on the site of the injection, which could be due to the anatomical parcellation of V2 (Fig. 5*A*). This is consistent with the interpretation that the layer 4B projection is part of the M stream and it suggests that its organization might be similar to that in monkeys.

We have also obtained information that relates to the organization of two additional streams: the B stream that in monkey flows through the blobs of V1 to the thin stripes of V2 and that processes color information, and the I stream that involves interblobs in V1 and the pale stripes in V2 and that performs color and form analysis. V1 injections restricted to interblobs have shown that the local projections from interblobs terminate preferentially in interblobs, whereas blob injections appear to label projections to nearby blobs and avoid interblobs. Thus, similar to the local connections in monkey V1 (29), the projections from the two different compartments do not appear to mix. This suggests that, as in monkeys, human blobs and interblobs might belong to different functional systems that may correspond to the B stream and the I stream, respectively, of nonhuman primates.

In summary, the results suggest that, as in monkey, the human visual system is composed of three functional streams that course through cortex. At present, knowledge about these pathways is incomplete, but based on results in nonhuman primates (33, 34) it is tempting to speculate that the M stream might continue from V1 to parietal cortex and the B and I streams to inferotemporal areas. Such an organization could explain why tasks that depend on the perception of visual motion such as smooth eye movements (35) are impaired in patients with posterior parietal lesions (36) and why damage to inferotemporal cortex results in the loss of color and form recognition (37–39).

We thank V. Charles for excellent technical assistance, Dr. R. Schmidt and J. Hardges for providing autopsy material, and T. A. Coogan and Dr. T. A. Woolsey for comments on the manuscript. This work was supported by National Institutes of Health Grant EY05935 (to A.B.).

1. DeYoe, E. A. & Van Essen, D. C. (1988) *Trends NeuroSci.* **11,** 219–226.
2. Livingstone, M. S. & Hubel, D. H. (1987) *J. Neurosci.* **7,** 3416–3468.
3. Glickstein, M. (1988) *Sci. Am.* **259,** 118–127.
4. Bailey, P. & von Bonin, G. (1951) *The Isocortex of Man* (Univ. of Illinois Press, Urbana).
5. Baillarger, J. G. F. (1840) *Mém. Acad. méd. Paris* **8,** 148.
6. Braak, H. (1977) *Anat. Embryol.* **150,** 229–250.
7. Brodmann, K. (1909) *Vergleichende Lokalisationslehre der Grosshirnrinde* (Barth, Leipzig, G. D. R.).
8. von Economo, C. (1929) *The Cytoarchitectonic of the Human Cerebral Cortex*, ed. Milford, H. (Oxford Univ. Press, London).
9. Hitchcock, P. F. & Hickey, T. L. (1980) *Brain Res.* **182,** 176–179.
10. Horton, J. C. & Hedley-Whyte, T. E. (1984) *Philos. Trans. R. Soc. London Ser. B* **304,** 255–272.
11. Hockfield, S. & Tootell, R. B. H. (1987) *Soc. Neurosci.* **13,** 3 (abstr.).
12. DeYoe, E. A. & Van Essen, D. C. (1985) *Nature (London)* **317,** 58–61.
13. Shipp, S. & Zeki, S. (1985) *Nature (London)* **315,** 322–324.
14. Godement, P., Vanselow, J., Thanos, S. & Bonhoeffer, F. (1987) *Development* **101,** 697–713.
15. McLean, I. W. & Nakane, P. K. (1974) *J. Histochem. Cytochem.* **22,** 1077–1083.
16. McCasland, J. S. & Woolsey, T. A. (1988) *J. Comp. Neurol.*, in press.
17. Holmes, G. M. (1918) *Br. J. Ophthalmol.* **2,** 353–384.
18. Wong-Riley, M. (1979) *Brain Res.* **171,** 11–28.
19. Blasdel, G. G., Lund, J. S. & Fitzpatrick, D. (1985) *J. Neurosci.* **5,** 3350–3369.
20. Tootell, R. B. H., Silverman, M. S. & DeValois, R. L. (1983) *Science* **220,** 737–739.
21. Rockland, K. S. (1985) *J. Comp. Neurol.* **235,** 467–478.
22. Beach, T. G. & McGeer, E. G. (1987) *Neurosci. Lett.* **76,** 37–41.
23. Beach, T. G. & McGeer, E. G. (1988) *J. Neurosci. Methods* **23,** 187–193.
24. Haber, S. (1988) *J. Neurosci. Methods* **23,** 15–22.
25. Livingstone, M. S. & Hubel, D. H. (1984) *J. Neurosci.* **4,** 309–356.
26. Hubel, D. H. & Livingstone, M. S. (1987) *J. Neurosci.* **7,** 3378–3415.
27. Rockland, K. S. & Pandya, D. N. (1979) *Brain Res.* **179,** 3–20.
28. Wong-Riley, M. (1979) *Brain Res.* **162,** 201–217.
29. Livingstone, M. S. & Hubel, D. H. (1984) *J. Neurosci.* **4,** 2830–2835.
30. Fox, P. T., Miezin, F. M., Allman, J. M., Van Essen, D. C. & Raichle, M. E. (1987) *J. Neurosci.* **7,** 913–922.
31. Petersen, S. E., Fox, P. T., Posner, M. I., Mintun, M. & Raichle, M. E. (1988) *Nature (London)* **331,** 585–589.
32. Posner, M. I., Petersen, S. E., Fox, P. T. & Raichle, M. E. (1988) *Science* **240,** 1627–1631.
33. Maunsell, J. H. R. & Van Essen, D. C. (1983) *J. Neurosci.* **3,** 2563–2586.
34. Livingstone, M. S. & Hubel, D. H. (1987) *J. Neurosci.* **7,** 3371–3377.
35. Van Essen, D. C. & Maunsell, J. H. R. (1983) *Trends NeuroSci.* **6,** 370–375.
36. Newsome, W. T., Wurtz, R. H., Dürsteler, M. R. & Mikami, A. (1985) *J. Neurosci.* **5,** 825–840.
37. Zihl, J., vonCramon, D. & Mai, N. (1983) *Brain* **106,** 313–340.
38. Damasio, A., Yamada, T., Damasio, H., Corbett, J. & McKee, J. (1980) *Neurology* **30,** 1064–1071.
39. Pearlman, A. L., Birch, J. & Meadows, J. C. (1979) *Brain* **106,** 313–340.